# Catalytic Activity of $CO_2$ Reduction on Pt Single-Crystal Electrodes: Pt(S)-[*n*(111)×(111)], Pt(S)-[*n*(111)×(100)], and Pt(S)-[*n*(100)×(111)]

**Nagahiro Hoshi,* Toshitake Suzuki, and Yoshio Hori***

*Department of Applied Chemistry, Faculty of Engineering, Chiba University 1-33, Yayoi-cho, Inage-ku, Chiba, 263, Japan*

*Received: April 15, 1997; In Final Form: August 10, 1997*[⊗]

The structural effect on the rate of $CO_2$ reduction was studied with voltammograms on Pt(S)-[*n*(111)×(100)] and Pt(S)-[*n*(100)×(111)] electrodes in 0.1 M $HClO_4$. The surfaces with higher step density gave higher rates of $CO_2$ reduction, as is the case of Pt(S)-[*n*(111)×(111)] reported previously. The electrodes with (111) step show higher activity for $CO_2$ reduction than those with (100) step. Pt(S)-[*n*(111)×(100)] and Pt(S)-[*n*(100)×(111)] give minimum rates at 0.25 V. This potential dependence differs remarkably from that on Pt(S)-[*n*(111)×(111)] on which the rates have maxima at 0.20 V. The following order of the activity for $CO_2$ reduction was obtained: Pt(S)-[*n*(111)×(100)] < Pt(S)-[*n*(100)×(111)] < Pt(S)-[*n*(111)×(111)]. Pt-(110) gave the highest rate of $CO_2$ reduction of all the examined surfaces. The atomic arrangement that enhances the activity for $CO_2$ reduction is discussed.

## Introduction

Relation between the catalytic activity and the atomic arrangement is highly important in the fundamental and the applied surface science. Catalytic reactions on single-crystal surfaces have been widely studied in gas phases,[1] such as ammonia synthesis, methanation and oxidation of CO, hydrolysis, and isomerization of hydrocarbons. Most of these studies are, however, limited to the low index planes. Somorjai et al. reported the orientation dependence of the selectivity and the reaction rate for hydrolysis and isomerization of hydrocarbons on high index planes of Pt. Structure of the terrace affects the selectivity of the reaction product of *n*-hexane hydrogenolysis[2] and butane isomerization,[3] and the presence of steps and kinks has an influence on the initial rates of isomerization of isobutane.[4] On the other hand, fewer papers have reported the catalytic reactions on single-crystal surfaces in liquid phases. Oxidation of small organic molecules (methanol, ethanol, butanol, and glucose) has been studied on the low index planes of Pt.[5] Some authors extended the study of the oxidation of formic acid to high index planes of Pt.[6−8] On the other hand, few reports have been published with regard to the electrochemical reduction on single crystals.

Electrochemical reduction of $CO_2$, one of the noteworthy reactions, can transform inert $CO_2$ to hydrocarbons and alcohols at room temperature and under atmospheric pressure.[9−11] Identification of the surface structure that enhances the rate of $CO_2$ reduction will contribute to the development of highly efficient catalysts reducing $CO_2$ with less energy. Pt electrodes reduce $CO_2$ to adsorbed product with adsorbed hydrogen atoms. The rate-determining step of this reaction is the hydrogen abstraction,[15] and an IRAS measurement identified the adsorbed product as CO.[16] Pt single crystals can be prepared easily in the laboratories,[17] and the amount of adsorbed CO can be obtained from its oxidation charge in the voltammogram. Electrochemical reduction of $CO_2$ on Pt single crystals is useful for studying the relationship between the reactivity and the surface structure, although it is not applied directly to the practical use.

Yeager et al. reported the reduction of $CO_2$ on low index planes of Pt for the first time.[18] Iwasita et al. extended the study to the high index planes.[19−21] However, the dynamics and the potential dependence of the reaction have not been studied in detail. We have been studying the atomic arrangement that enhances the rate of $CO_2$ reduction on various Pt single crystals.[22,23] The low index planes of Pt single crystals give the order of reactivity as follows: Pt(111) < Pt(100) < Pt(110).[18,19,22,24] The (110) surfaces of other Pt group metals (Ir, Rh, Pd) also have the highest activity for $CO_2$ reduction.[25−27] The most active Pt(110) has (111) step and (111) terrace, whereas the most inert Pt(111) is composed of atomically flat (111) terrace. We measured the rate of $CO_2$ reduction by changing the (111) step density on Pt(S)-[*n*(111)×(111)] single-crystal electrodes.[23] The rate of $CO_2$ reduction rises as the (111) step density increases. This result evidently shows that the (111) step raises the activity of $CO_2$ reduction.

This paper reports the structural effect and the potential dependence of the rate of $CO_2$ reduction at Pt(S)-[*n*(111)×(100)] and Pt(S)-[*n*(100)×(111)] electrodes. The results are compared with those on Pt(S)-[*n*(111)×(111)], and the possible active sites for $CO_2$ reduction are discussed.

## Experimental Section

Pt single crystals (3.5 mm Φ) were prepared from Pt wire (99.99%, 1 mm Φ) according to the method of Clavilier et al.[17] The crystals were oriented with the reflection beam of He−Ne laser from (111) and (100) facets[28] and polished with diamond slurry to optically flat surfaces. The surfaces were annealed in $H_2$−$O_2$ flame about 1300 °C and cooled in Ar + $H_2$ atmosphere before each voltammetric measurement. The electrodes used are given below:

$$\text{Pt(S)-[2(111)}\times\text{(100)]} = \text{Pt(S)-[2(100)}\times\text{(111)]} = \text{Pt(311)}$$

$$\text{Pt(S)-[3(111)}\times\text{(100)]} = \text{Pt(211)}$$

$$\text{Pt(S)-[4(111)}\times\text{(100)]} = \text{Pt(533)}$$

$$\text{Pt(S)-[9(111)}\times\text{(100)]} = \text{Pt(544)}$$

$$\text{Pt(S)-[3(100)}\times\text{(111)]} = \text{Pt(511)}$$

$$\text{Pt(S)-[4(100)}\times\text{(111)]} = \text{Pt(711)}$$

[⊗] Abstract published in *Advance ACS Abstracts,* October 1, 1997.

S1089-5647(97)01294-7 CCC: $14.00 

Pt(S)-[6(100)×(111)] = Pt(11 1 1)

Pt(S)-[9(100)×(111)] = Pt(17 1 1)

Pt(100)

Electrolytic solutions were prepared with ultrapure water treated with Milli Q low TOC (Millipore) and Suprapure grade chemicals (Merck). The purity of Ar and $CO_2$ were higher than 99.9999% and 99.999%, respectively. These gases were further deoxidized by passing through columns packed with activated copper. All the electrode potentials were referred to RHE and the experiments were conducted at 25 °C.

The activity of $CO_2$ reduction was estimated from the time course of the oxidation charge of adsorbed CO ($Q_{CO}$) in the voltammograms. The electrode potential was stepped from 0.5 V to a preset value $E_{ad}$ between 0.05 and 0.40 V (the adsorbed hydrogen region). Adsorbed hydrogen atoms reduce $CO_2$ to adsorbed CO at $E_{ad}$ for a given time $t_{ad}$. The potential was then stepped to 0.5 V and scanned at 0.05 V $s^{-1}$ to the positive direction in order to oxidize adsorbed CO.

## Results and Discussion

**1. Pt(S)-[*n*(111)×(100)] Electrodes.** Pt single crystals give voltammograms characteristic of their orientation between 0.05 and 0.60 V in 0.5 M $H_2SO_4$. Figure 1 shows voltammograms of Pt(S)-[*n*(111)×(100)] electrodes. The charges of the sharp peaks at 0.27 V equal the calculated oxidation charge of hydrogen adsorbed on the step, whereas those of the other peaks correspond to hydrogen atoms adsorbed on the terrace of 1 × 1 structure within the error of 10%. These results are identical with those reported by Clavilier et al.[29] and strongly support that the crystals are correctly oriented.

$CO_2$ was reduced in 0.1 M $HClO_4$, since $ClO_4^-$ does not interfere with the reaction between 0.05 and 0.40 V. The solution of $H_2SO_4$ was not used, since the adsorption of sulfuric acid anion ($HSO_4^-$ or $SO_4^{2-}$) prevents $CO_2$ reduction on Pt group metals.[26,30] The left-hand side of Figure 2 shows voltammograms of Pt(S)-[*n*(111)×(100)] electrodes in Ar saturated $HClO_4$. Redox peaks due to adsorbed hydrogen spread more positively than those in 0.5 M $H_2SO_4$. The right-hand side of Figure 2 gives the oxidation peaks of adsorbed CO after holding the potential at 0.05 V in $CO_2$ saturated $HClO_4$. The peak height grows with the increase of $t_{ad}$; the reduction of $CO_2$ proceeds on all the surfaces. We made control experiments in Ar-saturated $HClO_4$, confirming that no peak grows between 0.5 and 0.8 V after holding the potential at 0.05 V.

Figure 3 shows time courses of $Q_{CO}$ at 0.05 V, where a monolayer of adsorbed hydrogen atoms covers the electrode surface. $Q_{CO}$ rises steeply on highly stepped surfaces. We estimated the initial rate of $CO_2$ reduction $v_{t=0}$ from the slope of the tangential line at $t_{ad} = 0$.

Figure 4a shows $v_{t=0}$ plotted against $E_{ad}$. The order of $v_{t=0}$ coincides with that of the step density: Pt(544)($n = 9$) < Pt(533)($n = 4$) < Pt(211)($n = 3$) < Pt(311)($n = 2$). $CO_2$ was not reduced above 0.4 V where the Pt single-crystal electrodes adsorb no hydrogen atoms. Figures 4a reveals that the surfaces with higher (100) step density have higher activity for $CO_2$ reduction at any potential. The results on Pt(S)-[*n*(111)×(111)] reported previously[23] are reproduced in Figure 4b for comparison. We take the maximum value of $v_{t=0}$ as an index of the activity for $CO_2$ reduction. The maximum values of $v_{t=0}$ on Pt(S)-[*n*(111)×(100)] are lower than those on Pt(S)-[*n*(111)×(111)] with the same step density, as shown in Table 1. This result suggests that the (111) step is more effective for $CO_2$ reduction than the (100) step. The replacement of (111) step with (100) causes drastic changes in the potential dependence of $v_{t=0}$: Pt(S)-[*n*(111)×(100)] surfaces have minimum values of $v_{t=0}$ around 0.20 V where $v_{t=0}$'s on highly stepped Pt(S)-[*n*(111)×(111)] give maximum values.

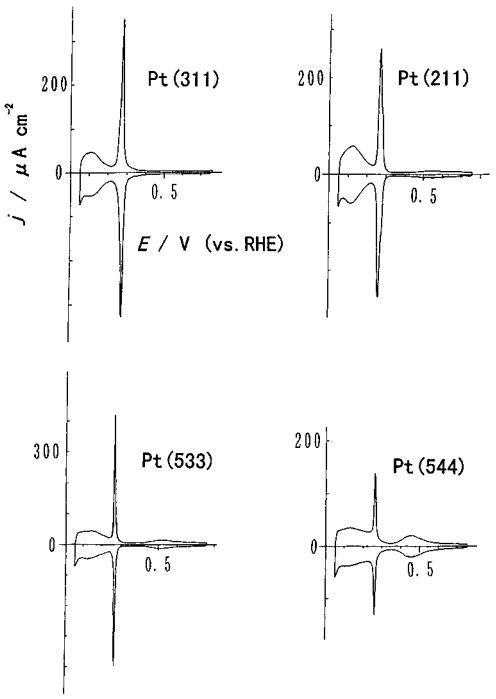


**Figure 1.** Voltammograms of Pt(S)-[*n*(111)×(100)] electrodes in 0.5 M $H_2SO_4$ solution saturated with Ar. Scanning rate: 0.05 V $s^{-1}$.

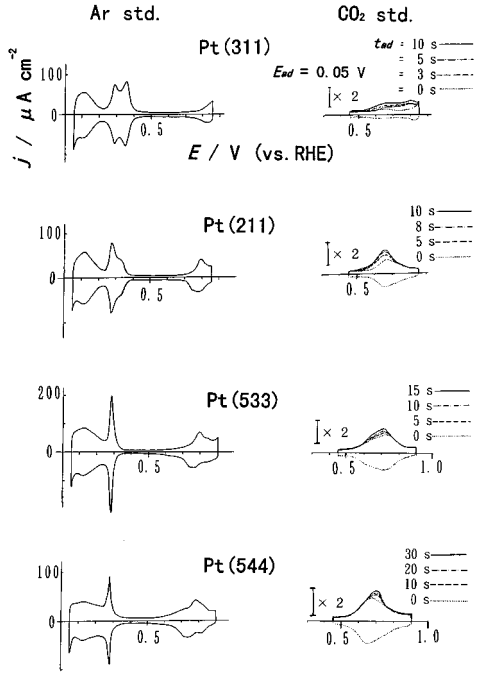


**Figure 2.** Voltammograms of Pt(S)-[*n*(111)×(100)] electrodes in 0.1 M $HClO_4$. Left-hand side: in Ar-saturated solution. Right-hand side: after holding the potential at 0.05 V for $t_{ad}$ in $CO_2$ saturated solution. Scanning rate: 0.05 V $s^{-1}$.

**2. Pt(S)-[*n*(100)×(111)] Electrodes.** Figure 5 shows voltammograms of Pt(S)-[*n*(100)×(111)] electrodes in 0.5 M $H_2SO_4$ saturated with Ar. The results of Pt(511), Pt(17 1 1), and Pt(100) are presented as representatives. Clavilier et al. and Feliu et al. reported that the peak at 0.37 V originates from wide (100) terrace (two-dimensional (100) structure), whereas the sharp peak at 0.27 V is attributed to (100) terrace edge (one-

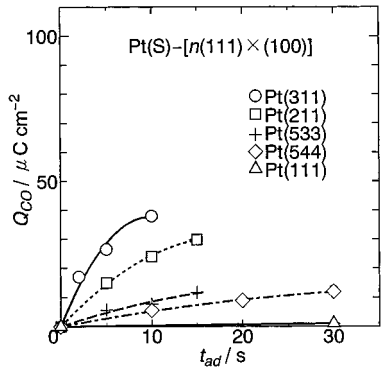


**Figure 3.** Time courses of adsorbed CO formation at 0.05 V on Pt-(S)-[$n$(111)×(100)] electrodes in 0.1 M $HClO_4$ saturated with $CO_2$.

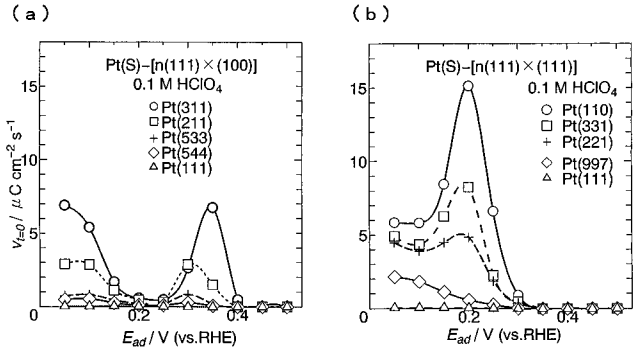


**Figure 4.** (a) Potential dependence of the initial rate of $CO_2$ reduction ($v_{t=0}$) on Pt(S)-[$n$(111)×(100)] in 0.1 M $HClO_4$. (b) Potential dependence of the $v_{t=0}$ on Pt(S)-[$n$(111)×(111)] in 0.1 M $HClO_4$.

**TABLE 1: Maximum Values of $v_{t=0}$[a]**

| | $v_{t=0}/\mu$C cm$^{-2}$ s$^{-1}$ | | |
|---|---|---|---|
| $n$ | $n$(111)×(111) | $n$(100)×(111) | $n$(111)×(100) |
| 2 | 15.2 | 6.9 | 6.9 |
| 3 | 8.3 | 3.9 | 2.9 |
| 4 | 4.8 | 3.5 | 0.8 |
| 6 | 2.5 | 2.4 | |
| 9 | 2.1 | 2.2 | 0.6 |
| ∞ | 0.07 | 3.2 | 0.07 |

[a] Pt(110)(1×1) is regarded as 2(111)×(111), although the structure of Pt(110) is not known at present.

dimensional (100) structure).[31,32] The peaks at 0.27 V get larger with the increase of step densities, whereas those at 0.37 V become greater with the increase of terrace width in Figure 5. The voltammograms agree with those reported by Motoo et al.[7] and Feliu et al.;[32] we judged that the crystals are correctly oriented.

Figure 6 presents voltammograms in 0.1 M $HClO_4$ saturated with $CO_2$. The redox peaks due to adsorbed hydrogen are broadened more positively than those in $H_2SO_4$, as is the case of Pt(S)-[$n$(111)×(100)]. All surfaces reduce $CO_2$ to adsorbed CO at 0.05 V, since the peaks of the CO oxidation develop with the increase of $t_{ad}$ in $CO_2$ saturated solution. Pt(17 1 1) and Pt(100) gave plateau peaks between 0.5 and 0.7 V in Ar-saturated $HClO_4$, not shown in Figure 6. These plateau peaks are not originated from adsorbed hydrogen that can reduce $CO_2$, since adsorbed CO was not formed after holding the potential between 0.5 and 0.7 V in $CO_2$ saturated $HClO_4$.

$Q_{CO}$ was plotted against $t_{ad}$, and $v_{t=0}$ was estimated from the tangential line at $t_{ad} = 0$. Figure 7 shows the potential dependence of $v_{t=0}$. The order of the activity for $CO_2$ reduction agrees with that of the step density between 0.05 and 0.4 V. Pt(100) is inert in this potential range but has higher activity at

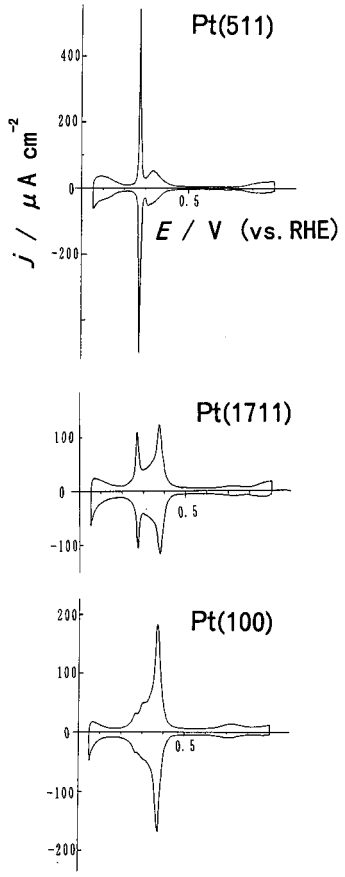


**Figure 5.** Voltammograms of Pt(S)-[$n$(100)×(111)] electrodes in 0.5 M $H_2SO_4$ saturated with Ar. Scanning rate: 0.05 V s$^{-1}$.

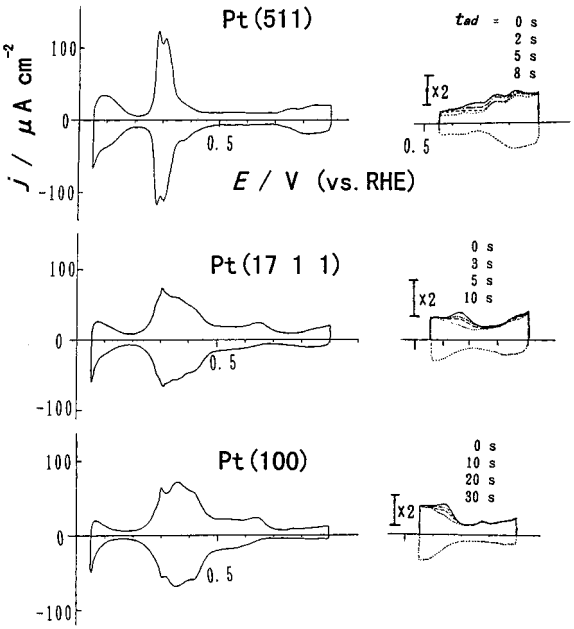


**Figure 6.** Voltammograms of Pt(S)-[$n$(100)×(111)] electrodes in $CO_2$-saturated M $HClO_4$. Left-hand side: normal voltammograms ($t_{ad}$ = 0). Right-hand side: after holding the potential at 0.05 V for $t_{ad}$ in $CO_2$-saturated solution. Scanning rate: 0.05 V s$^{-1}$.

0.45 V. This strange potential dependence of Pt(100) was also reported by Iwasita et al.[21] Weaver et al. reported that island-like structures appear on Pt(100) surface at positive potentials in $HClO_4$ containing CO.[33] Such island-like structures may be also formed in $HClO_4$ containing $CO_2$, providing active sites on Pt(100) at 0.45 V.

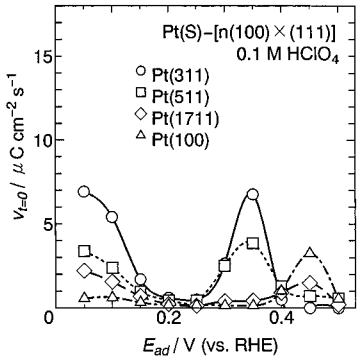


**Figure 7.** Potential dependence of the initial rate of $CO_2$ reduction ($v_{t=0}$) on Pt(S)-[$n$(100)×(111)] in 0.1 M $HClO_4$.

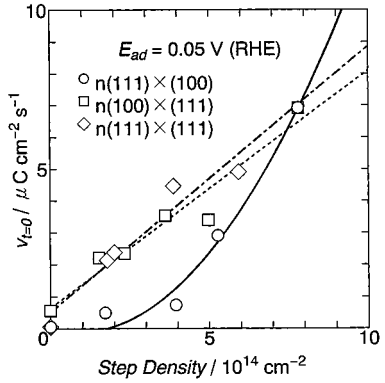


**Figure 8.** Step density dependence of the initial rate of $CO_2$ reduction ($v_{t=0}$) at 0.05 V in 0.1 M $HClO_4$.

The values of $v_{t=0}$ on Pt(S)-[$n$(100)×(111)] give minima at 0.25 V, as is the case of Pt(S)-[$n$(111)×(100)]. Maximum values of $v_{t=0}$ on highly stepped Pt(S)-[$n$(100)×(111)] are smaller than those on Pt(S)-[$n$(111)×(111)] with the same step density as shown in Table 1, even though both surfaces have (111) step. This fact shows that some factors other than the step structures may affect the activity for $CO_2$ reduction on Pt single crystals.

### 3. Effect of Atomic Arrangement

**3.1. Active Sites at 0.05 V.** All the adsorption sites of hydrogen are fully occupied at 0.05 V. The values of $v_{t=0}$ at 0.05 V are plotted against the step density in Figure 8. The surfaces with (111) step apparently have higher activity for $CO_2$ reduction than those with (100) step at 0.05 V. The plots for Pt(S)-[$n$(111)×(100)] may be correlated with square of the step density. On the other hand, $v_{t=0}$ depends linearly on the (111) step density on both Pt(S)-[$n$(111)×(111)] and Pt(S)-[$n$(100)×(111)]. The plots for Pt(S)-[$n$(100)×(111)] trace almost the same line as those of Pt(S)-[$n$(111)×(111)]. This fact strongly suggests that Pt(S)-[$n$(100)×(111)] and Pt(S)-[$n$(111)×(111)] have common active sites for $CO_2$ reduction at 0.05 V.

The adsorption sites of hydrogen are important as the active sites on Pt single crystals, since the process involved with adsorbed hydrogen is the rate-determining step of the $CO_2$ reduction on Pt electrodes.[15] IRAS[34,35] and sum frequency generation measurements[36,37] detected terminal hydrogen adsorbed on Pt electrodes in aqueous phase. However, the potential dependence of the band intensity obtained in these spectroscopic measurements does not agree with that of oxidation charge of adsorbed hydrogen in voltammograms. The surfaces we examined (Pt(110) and Pt(11 1 1)) adsorb no terminal hydrogen between 0.05 and 0.5 V in accordance with Ogasawara et al.[35] Thus, we do not discuss the contribution of terminal hydrogen to the reduction of $CO_2$ in this paper any more.

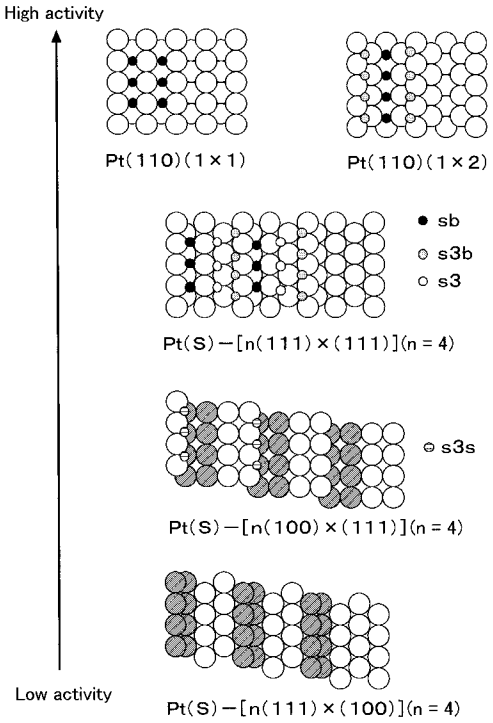


**Figure 9.** Atomic arrangements and possible adsorption sites of hydrogen on various single crystals. Small dark circles: bridge site in the 4-fold atomic arrangement in the step ($s_b$). Small shaded circles: 3-fold hollow site on top of the step ($s_{3b}$). Small striped circles: 3-fold hollow site at the step ($s_{3s}$). Small open circles: 3-fold hollow site in the flat terrace ($s_3$). Large shaded circles: one-dimensional (100) structure.

The redox peaks of the hydrogen atoms in the voltammograms will be closely related with the adsorption sites. The relation is not, however, fully revealed at present. Furthermore, the atomic arrangements of Pt high index planes have not been directly observed with STM in aqueous solution, although the charges of the voltammograms indicate the surfaces composed of 1 × 1 structure.[29,38] We discuss the active sites for $CO_2$ reduction with the following assumptions: (1) The hydrogen adsorption sites in liquid phase are identical to those shown under UHV. (2) High index planes of Pt have 1 × 1 structure.

Figure 9 shows possible adsorption sites of hydrogen on the various atomic arrangements of the surfaces. Although Pt(S)-[$n$(111)×(111)] and Pt(S)-[$n$(100)×(111)] surfaces apparently have (111) steps, the adsorption sites of hydrogen around the steps are different. Pt(S)-[$n$(111)×(111)] surfaces adsorb hydrogen at bridge site ($s_b$) in the pseudo-4-fold atomic arrangement in the step and at the 3-fold hollow site ($s_3$) in the terrace under UHV.[39] The hydrogen atoms adsorbed at $s_3$ in the flat (111) terrace have the low activity for $CO_2$ reduction.[22,23] However, hydrogen atoms on top of the step ($s_{3b}$) may have especially higher activity for $CO_2$ reduction than those at the flat terrace on Pt(S)-[$n$(111)×(111)]; hydrogen atoms at $s_{3b}$ have the opposite sign of dipole moment to the other ones at the flat terrace on Pt(S)-[9(111)×(111)].[40] On the other hand, Pt(S)-[$n$(100)×(111)] surfaces have no pseudo-4-fold atomic arrangement in the step. Hydrogen will be adsorbed at $s_3$ in the (111) step ($s_{3s}$) and the bridge or 4-fold hollow sites ($s_4$) in the (100) terrace.[41] The $s_{3s}$ is the only site that has the symmetry identical to $s_3$ on Pt(S)-[$n$(111)×(111)]. Therefore, $s_{3b}$ of Pt(S)-[$n$(111)×(111)] and $s_{3s}$ of Pt(S)-[$n$(100)×(111)] may be the common active sites for $CO_2$ reduction at 0.05 V.

**3.2. $CO_2$ Reduction at the Potentials Higher than 0.05 V.** Next, we discuss the effect of surface structures on $v_{t=0}$ at the potentials higher than 0.05 V, where the coverage of hydrogen is less than 1. The active sites in this potential range probably differ from those at 0.05 V, since the potential dependence of $v_{t=0}$ on Pt(S)-[$n$(100)×(111)] contrasts with that on Pt(S)-[$n$(111)×(111)] above 0.05 V. The plots of $v_{t=0}$ against $E_{ad}$ on Pt(S)-[$n$(100)×(111)] resemble those on Pt(S)-[$n$(111)×(100)] qualitatively, as shown in Figures 4 and 7: both Pt(S)-[$n$(111)×(100)] and Pt(S)-[$n$(100)×(111)] give minimum values of $v_{t=0}$ at 0.25 V. Both Pt(S)-[$n$(111)×(100)] and Pt-(S)-[$n$(100)×(111)] surfaces have one-dimensional (100) structure in the step and the terrace edge, respectively, whereas Pt(S)-[$n$(111)×(111)] surfaces possess no such structure, as shown in Figure 9. These results suggest that one-dimensional (100) structure at the step and the terrace edge deactivates the $CO_2$ reduction around 0.25 V, although the mechanism is not known at the present stage. On the other hand, especially high values of $v_{t=0}$ at 0.20 V on highly stepped Pt(S)-[$n$(111)×(111)] may originate from the $s_b$ that does not exist on the other surfaces. It is necessary to observe actual surface structure with in situ STM for discussing the potential dependence of $v_{t=0}$ in more detail.

Maximum values of $v_{t=0}$ on the surfaces with the same step densities determine the order of the catalytic activity of $CO_2$ reduction as follows: Pt(S)-[$n$(111)×(100)] < Pt(S)-[$n$(100)×(111)] < Pt(S)-[$n$(111)×(111)]. Pt(110) has the highest activity of $CO_2$ reduction in the examined surfaces. Although we do not know whether Pt(110) has 1 × 1 or 1 × 2 structure in aqueous phase, both structures have symmetrical $s_b$ that does not exist on the other surfaces, as shown in Figure 9. Such symmetrical $s_b$ may be the structure that reduces $CO_2$ most efficiently.

## Conclusion

1. The initial rate of $CO_2$ reduction rises with the increase of step density on Pt(S)-[$n$(111)×(100)] and Pt(S)-[$n$(100)×(111)] electrodes, as is the case of Pt(S)-[$n$(111)×(111)].

2. The initial rates of $CO_2$ reduction on Pt(S)-[$n$(111)×(100)] and Pt(S)- [$n$(100)×(111)] give minimum values at 0.25 V. This potential dependence remarkably differs from that on Pt(S)-[$n$(111)×(111)] on which the initial rates yield maximum at 0.20 V.

3. The surfaces with (111) steps reduce $CO_2$ more efficiently than those with (100) step.

4. The order of the activity for $CO_2$ reduction is the following: Pt(S)-[$n$(111)×(100)] < Pt(S)-[$n$(100)×(111)] < Pt(S)[$n$(111)×(111)]. Pt(110) has the highest activity for $CO_2$ reduction.

**Acknowledgment.** This study was supported by grant in aids of Scientific Research, No. 08740440 and No. 08232217.

## References and Notes

(1) Rodriguez, J. A.; Goodman, D. W. *Surf. Sci. Rep*. **1991**, *14*, 1 and references therein.
(2) Davis, S. M.; Zaera, F.; Somorjai, G. A. *J. Catal*. **1982**, *104*, 7453.
(3) Davis, S. M.; Zaera, F.; Somorjai, G. A. *J. Am. Chem. Soc*. **1982**, *104*, 7453.
(4) Zaera, F; Somorjai, G. A. *Langmuir* **1986**, *2*, 686.
(5) Lamy, C; Leger, J. M. *J. Chim. Phys.* **1991**, *88*, 1649 and references threrein.
(6) Adzic, R. R.; Tripkovic A. V.; Vesovic, V. B. *J. Electroanal. Chem.* **1986**, *204*, 329.
(7) Motoo, S.; Furuya, N. *Ber. Bunsen-Ges. Phys. Chem.* **1987**, *91*, 457.
(8) Sun, S.-F.; Lin, Y.; Li. N.-H.; Mu, J.-Q. *J. Electroanal. Chem*. **1994**, *370*, 273.
(9) Hori, Y.; Kikuchi, K.; Suzuki, S. *Chem. Lett*. **1985**, 1965.
(10) Hori, Y.; Murata, A.; Takahashi, R. *J. Chem. Soc., Faraday Trans. 1* **1989**, *85*, 2309.
(11) Hori, Y.; Wakabe, H.; Tsukamoto, T.; Koga, O. *Electrochim. Acta* **1994**, *39*, 1833 and references therein.
(12) Giner, J. *Electrochim. Acta* **1963**, *8*, 857.
(13) Breiter, M. W. *Electrochim. Acta* **1967**, *12*, 1213.
(14) Arevalo, M. C.; Gomis-Bas. C.; Hahn, F.; Beden, B.; Arevalo, A.; Arvia, A. J. *Electrochim. Acta* **1994**, *39*, 793. and references therein.
(15) Sobkowski, J.; Czerwinski, A. *J. Electroanal. Chem.* **1975**, *65*, 327.
(16) Beden, B.; Bewick, A.; Razaq, M.; Weber, J. *J. Electroanal. Chem.* **1982**, *139*, 203.
(17) Clavilier, J.; Faure, R.; Guinet, G.; Durand, R. *J. Electroanal. Chem.* **1980**, *107*, 205.
(18) Nicholic, B. Z.; Huang, H.; Gervasio, D.; Lin, A.; Fierro, C.; Adzic, R. R.; Yeager, E. B. *J. Electroanal. Chem.* **1990**, *295*, 415.
(19) Rodes, A.; Pastor, E.; Iwasita, T. *J. Electroanal. Chem.* **1994**, *369*, 183.
(20) Rodes, A.; Pastor, E.; Iwasita, T. *J. Electroanal. Chem.* **1994**, *373*, 167.
(21) Rodes, A.; Pastor, E.; Iwasita, T. *J. Electroanal. Chem.* **1994**, *377*, 215.
(22) Hoshi, N.; Mizumura, T.; Hori, Y. *Electrochim. Acta* **1995**, *40*, 883.
(23) Hoshi, N.; Suzuki, T.; Hori, Y. *Electrochim. Acta* **1996**, *41*, 1647.
(24) Taguchi, S.; Aramata, A. *Electrochim. Acta* **1994**, *39*, 2533.
(25) Hoshi, N.; Uchida, T.; Mizumura, T.; Hori, Y. *J. Electroanal. Chem.* **1995**, *381*, 261.
(26) Hoshi, N.; Ito, H.; Suzuki, T.; Hori, Y. *J. Electroanal. Chem.* **1995**, *395*, 309.
(27) Hoshi, N.; Noma, M.; Suzuki, T.; Hori, Y. *J. Electroanal. Chem.* **1997**, *421*, 15.
(28) Motoo, S.; Furuya, N. *J. Electroanal. Chem.* **1984**, *172*, 339.
(29) Rodes, A.; El Achi, K.; Zamakhchari, M. A.; Clavilier, J. *J. Electroanal. Chem.* **1990**, *284*, 245.
(30) Hoshi, N.; Suzuki, T.; Hori, Y. *J. Electroanal. Chem*. **1996**, *416*, 65.
(31) Clavilier, J.; Armand, D. *J. Electroanal. Chem.* **1986**, *199*, 187.
(32) Feliu, J. M.; Rodes, A.; Orts, J. M.; Clavilier, J. *Polish J. Phys. Chem.* **1994**, *68*, 1575.
(33) Vitus, C. M.; Chang, S.-C.; Schardt, B. C.; Weaver, M. J. *J. Phys. Chem.* **1991**, *95*, 7559.
(34) Nichols, R. J.; Bewick, A. *J. Electroanal. Chem.* **1988**, *243*, 445.
(35) Ogasawara, H.; Ito, M. *Chem. Phys. Lett.* **1994**, *221*, 213.
(36) Peremans, A.; Tadjeddine, A. *J. Chem. Phys*. **1995**, *103*, 7197.
(37) Tadjeddine, A.; Peremans, A. *J. Electroanal. Chem.* **1996**, *409*, 115 and references therein.
(38) Clavilier, J.; Rodes, A. *J. Electroanal. Chem*., **1993**, *348*, 247 and references therein.
(39) Baro, A. M.; Ibach, H. *Surf. Sci*. **1980**, *92*, 237.
(40) Christman, K.; Ertl, G. *Surf. Sci*. **1976**, *60*, 365.
(41) Zinola, C. F.; Arvia, A. J. *Electrochim. Acta* **1996**, *41*, 2267.